HEMATOPOIESIS AND STEM CELLS

Inflammatory signaling regulates hematopoietic stem and progenitor cell emergence in vertebrates

Qiuping He, Chunxia Zhang, Lu Wang, Panpan Zhang, Dongyuan Ma, Junhua Lv, and Feng Liu

State Key Laboratory of Biomembrane and Membrane Biotechnology, Institute of Zoology, Chinese Academy of Sciences, Beijing, China

Key Points

- TLR4–MyD88–NF-κB is required for HSPC emergence in zebrafish and mouse embryos.
- Notch functions downstream of inflammatory signaling to regulate HSPC emergence.

Inflammatory signaling has been shown to be essential for stress hematopoiesis in adult bone marrow, either through increasing proliferation or by directing differentiation of hematopoietic stem and progenitor cells (HSPCs) toward myeloid or lymphoid lineages. However, its role in embryonic normal hematopoiesis has been unknown. Here, we demonstrate that in both zebrafish and mouse embryos, inflammatory signaling is necessary and sufficient for HSPC emergence, in the absence of infection or pathological inflammation. Mechanistically, inflammatory signaling regulates hemogenic endothelium-derived HSPC development through a conserved Toll-like receptor 4 (TLR4)–nuclear factor κ-light-chain enhancer of activated B core (NF-κB) signaling, which then promotes Notch activity, a well-known signal required for HSPC specification in vertebrates. Our findings establish a previously unrecognized link between inflammatory signaling and HSPC emergence, and provide new insights into regenerative medicine and novel therapies to treat innate immune-related diseases. (*Blood*. 2015;125(7):1098-1106)

Introduction

Hematopoietic stem cells (HSCs) have the abilities of self-renewal and multilineage differentiation to maintain the supply of all mature blood cells for the lifetime. In vertebrate embryos, the earliest definitive hematopoietic stem and progenitor cells (HSPCs) are originated from a group of specialized endothelial cells, hemogenic endothelium (HE),[1-4] through the endothelial-to-hematopoietic transition (EHT) process.[5-7] In vitro generation and/or expansion of functional and transplantable bona fide HSCs with self-renewal and multilineage potential hold great promise in regenerative medicine. However, this has not been achieved yet, at least partially because a complex interplay between cell-extrinsic cues and cell-intrinsic regulatory signaling governing HE formation and HSPC specification remains incompletely understood.

Inflammatory signaling is generally thought to be active in the presence of infection and inflammation. In response to infection stimuli, innate immune cell–secreted inflammatory cytokines directly or indirectly act on myeloid precursors to differentiate and expand to meet the acute demand of effector myeloid cells. However, recent reports also showed that inflammatory cytokine can also directly act on HSPCs to instruct their fate, either increased proliferation or directed differentiation toward myeloid[8] or lymphoid[9] lineages, at the expense of HSC self-renewal and/or maintenance in the bone marrow.[10,11] Upon Toll-like receptor (TLR) stimulation, nuclear factor κ-light-chain enhancer of activated B (NF-κB), a central player in innate immune response, integrates multiple inflammatory signaling pathways including tumor necrosis factor α (TNFα) and granulocyte colony-stimulating factor (G-CSF) pathways. NF-κB has been shown to regulate both innate and adaptive immune systems including myeloid cells and B and T cells in homeostasis and differentiation. Interestingly, the role of inflammatory signals during HSPC emergence in both zebrafish and mouse embryos has been described very recently.[12-14]

Inflammatory signaling pathways are well conserved in vertebrates. Previous studies in mice showed that cytokines including interleukin-1 (IL-1) and IL-3 are involved in the embryonic development of HSPCs in the aorta-gonad-mesonephros (AGM) region.[15,16] We previously reported that a hematopoietic microRNA, *miR-142a-3p*, regulates the formation and differentiation of HSPCs by regulating the inflammatory signaling cascade *irf7-gcsfr*,[17] indicating a possible role of inflammatory signaling in HSPC emergence. In this study, we demonstrated that in both zebrafish and mouse embryos, inflammatory signaling is required for HSPC specification. Ablation of the TLR4–myeloid differentiation primary response 88 (MyD88) pathway and inflammatory cytokine signaling pathways including TNFα and G-CSF, decreased the population of the earliest HSPCs through downregulation of their core effector NF-κB, which in turn reduced the Notch activity in endothelial cells. Attenuation of Notch activity in endothelial cells then compromised the HE and the following HSPC emergence via the EHT process. Therefore, we discovered, for the first time, an unexpected essential role of proinflammatory signaling in HSPC emergence through a conserved NF-κB–Notch pathway.

Submitted September 15, 2014; accepted December 22, 2014. Prepublished online as *Blood* First Edition paper, December 24, 2014; DOI 10.1182/blood-2014-09-601542.

Q.H., C.Z., and L.W. contributed equally to this work.

The online version of this article contains a data supplement.

The publication costs of this article were defrayed in part by page charge payment. Therefore, and solely to indicate this fact, this article is hereby marked "advertisement" in accordance with 18 USC section 1734.

Methods

Fish strains and embryos

Zebrafish strains including Tubingen, *cmyb*:green fluorescent protein (GFP),[18] *kdrl*:mCherry,[5] *fli1a*:enhanced GFP (EGFP),[19] heat shock protein (HSP)-*il1b*-EGFP,[20] *CD41*:GFP,[21] *mpo*:GFP,[22] *lyz*:DsRed,[23] *myd88* mutants,[24] *tp1*:DsRed,[25] and *runx1*:en-GFP (P.Z. and F.L., manuscript in preparation) were raised and maintained in system water at 28.5°C. The HSP-*il1b*-EGFP embryos were heat-shocked from 20 hours post fertilization (hpf) for 30 minutes at 42°C. The embryos were obtained by natural spawning. This study was approved by the Ethical Review Committee in the Institute of Zoology, Chinese Academy of Sciences, China.

Morpholinos and microinjection

Antisense Morpholinos (MOs) used in this study (including *runx1* MO,[7] *tlr4bb* MO,[26] *myd88* MO,[27] *tnfr2* MO,[28] *gcsfr* MO,[29] *ikbaa* MO, *pu.1* MO,[30] *irf8* MO,[31] *cebp1* MO,[32] mismatch MOs (mis MOs), and standard control MO) were purchased from GeneTools and dissolved with distilled H_2O into 1 mM as stock solutions. MOs (4 ng for *runx1* MO; 1 ng for *tlr4bb* MO and *tlr4bb* mis MO; 2 ng for *ikbaa* MO and *ikbaa* mis MO; 4 ng for *myd88* MO and *myd88* mis MO; 3 ng for *tnfr2* MO and *tnfr2* mis MO; 8 ng for *gcsfr* MO; 6 ng for *pu.1* MO; 6.4 ng for *irf8* MO; 4 ng for *cebp1* MO and 8 ng for control MO) were injected into 1-cell-stage zebrafish embryos at the yolk/blastomere boundary. The MO sequences are listed in supplemental Table 1 (available on the *Blood* Web site). For overexpression of dominant-negative *ikbaa* (*dnikbaa*) or *NICD* specifically in the blood vessel region, the zebrafish *ikbaa* lacking the first 117 N-terminal nucleotides or full-length coding sequences of zebrafish *NICD* were cloned into pDONR221 vector by attB and attP recombination reaction (Gateway System) to generate the entry clones, and then subcloned into a pDestTol2pA2 vector with P5E-*fli1*ep (*fli1* enhancer/promoter)[33] and p3E-V2AEGFP-pA by attL and attR recombination reaction (MultiSite Gateway Technology; Invitrogen). The pEGFP-N1-*ikbaa* fusion construct containing the *ikbaa* MO recognition site was coinjected with both *ikbaa* MO and *ikbaa* mis MO.

Whole-mount in situ hybridization

Whole-mount in situ hybridization (WISH) for embryos was performed using the ZF-A4 in situ hybridization machine (Zfand) with probes including *runx1*, *cmyb*, *rag1*, *foxn1*, *ephrinB2*, *gata1*, *scl*, and *kdrl*.[34-36]

RNA-seq and GO analysis

The trunk region of Tg(*runx1*:en-GFP) embryos at 26 to 28 hpf was dissected to sort the GFP^+ cells for RNA-Seq. The *runx1* GFP^+ cells were sorted by AriaI (BD Biosciences). Total RNA from the sorted cells was purified and subjected to RNA-Sequencing (RNA-Seq). Beijing Genomics Institute provided the deep-sequencing service and subsequent gene ontology (GO) analysis.

Chemical treatment

Embryos were treated with dimethylsulfoxide (AMRESCO) or JSH-23 (300 μM; Selleck) from 10-somite stage to 24 hpf or 36 hpf.

Quantitative RT-PCR

Total RNA from trunk region of zebrafish embryos and the AGM regions of $tlr4^{+/-}$ and $tlr4^{-/-}$ mouse embryos at embryonic day 10.5 (E10.5) were extracted by TRNzol Reagent (Tiangen) and were reversely transcribed using reverse transcriptase (RT). The complementary DNA was diluted 5 times as the templates. Quantitative polymerase chain reaction (qPCR) was performed with GoTaq qPCR Master Mix (Promega) using the Bio-Rad CFX96 Real-Time PCR system. The PCR primers used are listed in supplemental Table 2.

Western blot

The trunk regions of zebrafish embryos were dissected for the protein extraction. The nuclear protein was extracted using the Nucl-Cyto-Mem Preparation kit (Applygen). The whole-cell protein extraction and western blot were performed as previously reported[34] using anti-p65 (1:800; Cell Signaling Technology), anti-pIκBα (1:800; Cell Signaling Technology), anti-LaminB1 (1:4000; Abcam), and anti-Tubulin β (1:1000; Proteintech) antibodies.

TUNEL assay and BrdU labeling

TUNEL (terminal deoxynucleotidyltransferase-mediated dUTP nick end labeling) and BrdU (5-bromo-2′-deoxyuridine) assays were performed as described previously.[37]

Tail amputation assay

The tail fin of Tg(*mpo*:GFP) embryos was cut at 24 hpf as described previously.[20]

Confocal microscopy

Confocal images were acquired as previously reported[38] with a Nikon confocal A1 laser microscope, and 3-dimensional projections were generated using Nikon confocal software. The supplemental Videos from 33 to 54 hpf were generated with PerkinElmer spinning disk confocal microscopy[38] and edited by ImageJ.

Zebrafish embryo dissociation and FACS

Embryo dissociation and fluorescence-activated cell sorter (FACS) were performed as described previously.[39] The $cmyb^-kdrl^+$ and $cmyb^+kdrl^+$ cells were separately collected from *cmyb*:GFP/*kdrl*:mCherry transgenic embryos and lyz^+ cells from *lyz:*DsRed transgenic embryos using AriaI (BD Biosciences).

Inhibition of transcription using dead-Cas9-KRAB

The plasmid with the full length of a human codon-optimized, catalytically inactive version of Cas9 (dCas9), fused with Krüppel-associated box (KRAB) repressor domain, was kindly provided by Liu Dong (Peking University). Capped dCas9-KRAB messenger RNA was synthesized using the mMessage mMachine T7 kit (Ambion) and purified with an RNA purification kit (Tiangen). The guide RNAs (gRNAs) for zebrafish genes were designed according to the Web site (http://zifit.partners.org/ZiFiT/), synthesized by T7 RNA polymerase, and purified by the mirVanaTM miRNA Isolation kit (Ambion) in vitro. Five different gRNAs targeting the downstream transcription start site at the antisense strand were designed for each gene to inhibit the transcription elongation. Cas9 messenger RNA (200 ng/μL) and 5 gRNAs (100 ng/μL per gRNA) were coinjected into 1-cell stage wild-type embryos. Injected embryos were incubated at 28.5°C and collected for quantitative RT-PCR (qRT-PCR), confocal imaging, and WISH at different stages.

Immunofluorescence

An immunofluorescence assay for mouse embryos was performed as previously reported.[34] $tlr4^{+/-}$ and $tlr4^{-/-}$ embryos at E10.5 were fixed with 4% paraformaldehyde in phosphate-buffered saline for 6 to 8 hours at 4°C. The slides were blocked with 5% bovine serum albumin for 1 hour at room temperature and incubated with Runx1 (Abcam) antibody diluted in 1% bovine serum albumin overnight at 4°C. After being washed 3 times in phosphate-buffered saline with Tween 20, the slides were incubated with anti-rabbit-immunoglobulin-fluorescein for 1 hour at room temperature. The sections were counterstained with 4,6 diamidino-2-phenylindole and images were acquired by Nikon confocal A1.

Mouse embryo dissociation and FACS

E10.5 AGMs (36-40 somite pairs) were dissociated by collagenase. FACS was performed as previously reported[34] using MoFlo XDP. The $CD31^+CD41^-CD45^-TER119^-$ cells of the indicated numbers from $tlr4^{+/-}$ or $tlr4^{-/-}$ were cultured on mouse OP9 stromal cells and supplemented with hematopoietic cytokines (50 ng/mL stem cell factor, 50 ng/mL IL3, 20 ng/mL FLT3 ligand). After being cultured for 4 days, semiadherent cells were carefully harvested for flow cytometry.

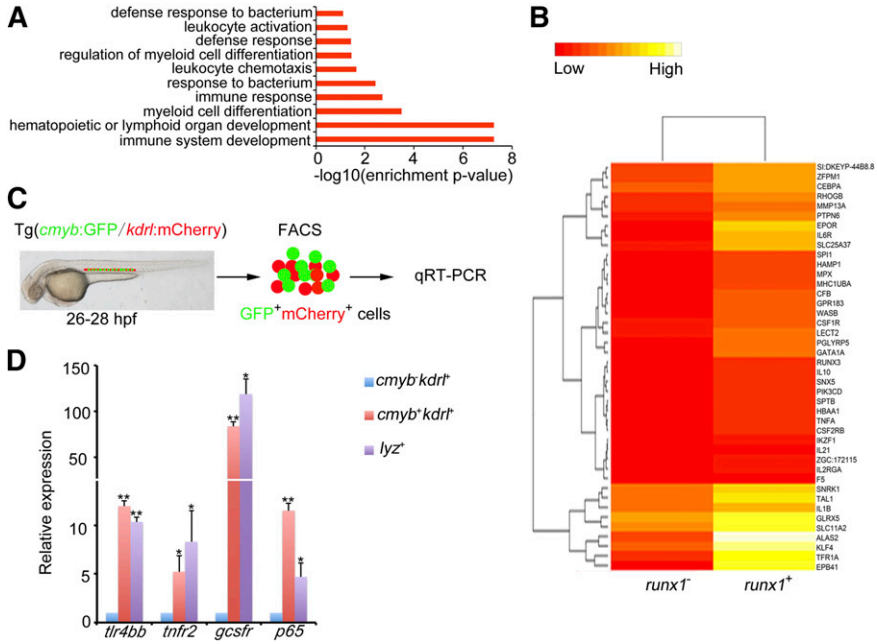

Figure 1. Inflammatory signaling is enriched in hemogenic endothelium. (A) *runx1* GFP$^+$ cells from Tg(*runx1*:en-GFP) transgenic embryos at 26 to 28 hpf were sorted for deep sequencing. The GO analysis of the sequencing data identified that inflammatory signaling was enriched in *runx1*$^+$ cells. (B) Heat map analysis showed comparison of gene expression between *runx1* GFP$^+$ and *runx1* GFP$^-$ cells at 26 to 28 hpf. Multiple inflammatory signaling genes were found enriched in GFP$^+$ cells. (C) *cmyb*$^-$*kdrl*$^+$ and *cmyb*$^+$*kdrl*$^+$ cells from Tg(*cmyb*:GFP/*kdrl*:mCherry) embryos were sorted at 26 to 28 hpf, and *lyz*$^+$ cells from Tg(*lyz*:DsRed) embryos were sorted at 48 hpf. (D) qRT-PCR results showed that a panel of inflammatory signaling genes was enriched in *cmyb*$^+$*kdrl*$^+$ hemogenic endothelial cells. Each bar represents the mean ± SEM of 3 independent samples. *$P < .05$, **$P < .01$.

CFC assay

A colony-forming cell (CFC) assay was performed as previously reported.[34] The experiment was repeated in triplicate.

Flow cytometric analysis

Semiadherent cells were carefully harvested. Then, antibody staining was performed as described previously,[34] using antibodies specific to C-Kit–phycoerythrin [PE]–CY7, CD45-PE, CD45.2-PE-CY7, Gr1-PE, CD3–fluorescein isothiocyanate, B220, CD4–fluorescein isothiocyanate, and CD8a-PE (eBioscience).

HSC transplantation assay

Eight-week-old male CD45.1 mice were exposed to a split dose of 9 Gy x-ray irradiation. The 2 embryo equivalent cells from *tlr4*$^{+/-}$ (CD45.2) or *tlr4*$^{-/-}$ (CD45.2) AGM regions were injected into irradiated adult recipients via tail vein, together with 20 000 CD45.1 bone marrow cells. Bone marrow, spleen, and thymus of recipients were collected at the indicated time points. Greater than 10% CD45.2-positive cells as determined by flow cytometry was considered successful reconstitution.

Statistical analysis

All experiments were performed at least 3 times. Data were given as the mean ± standard error of the mean (SEM). The Student *t* test was used for statistical comparisons.

Results

Expression of inflammatory signaling in HE and HSPCs

Previous studies in zebrafish and mouse embryos[15-17] implicate the potential involvement of inflammatory signaling in HSPC emergence. To further test this possibility, we examined the expression profiling of the earliest HSPC population in zebrafish embryos. A mouse *runx1* intronic enhancer was used to drive GFP in zebrafish embryos which can mimic zebrafish *runx1* endogenous expression.[40] The newly generated *runx1*:en-GFP line can faithfully mark the earliest HSPCs in zebrafish embryos (supplemental Figure 1). We first performed RNA-Seq with hemogenic endothelial cells by isolating *runx1*$^+$ GFP cells (P.Z. and F.L., manuscript in preparation) using FACS at 26 to 28 hpf, at which stage the hemogenic endothelial cells were just specified and underwent the EHT in the ventral wall of the dorsal aorta.[5,7,41] Interestingly, GO analysis showed that inflammatory signaling was highly enriched among the upregulated genes in *runx1*$^+$ cells (Figure 1A-B). The qRT-PCR result confirmed the RNA-Seq data (Figure 1C). Notably, the sorted hemogenic endothelial cells expressed a high level of inflammatory signaling components including cytokine receptors and NF-κB3 (p65); the myeloid cells were used as the positive control (Figure 1D). Together, these data strongly suggest that inflammatory signaling transduced by HE and HSPCs might be involved in definitive hematopoiesis in zebrafish.

Loss of function of TLR4–MyD88–NF-κB leads to HSPC defects

To investigate whether proinflammatory signaling is required for HSPC specification, we first performed loss-of-function experiments for the core of inflammatory signaling players, the TLR4–MyD88–NF-κB axis.[42] The AGM expression of *runx1*, which is a well-known HSPC marker in zebrafish and mammals, was drastically reduced in *tlr4bb* or *myd88* morphants (Figure 2A, supplemental Figure 2A-B). Additionally, the number of *cmyb*:GFP/*kdrl*:mCherry double-positive HSPCs[5] in the AGM region was significantly reduced in *tlr4bb*- or *myd88*-deficient embryos, compared with control embryos (Figure 2B, supplemental Figure 2C). The number of *CD41*$^+$ cells, that is, the hematopoietic progenitor cells, was also significantly reduced in deficient embryos at 48 hpf (Figure 2C). A well-known readout for HSPC function in zebrafish is its capability to differentiate into T lymphoid. We thus examined expression of T-cell marker *rag1*. WISH showed that *rag1* expression was remarkably reduced in *tlr4bb* or *myd88* morphants, whereas the expression of thymic epithelial cell marker *foxn1* was normal (Figure 2A), further supporting that T-cell defects in these deficient embryos resulted from early HSPC defects. We further used the newly developed clustered regularly interspaced short palindromic repeats (CRISPR)/Cas9 technology to manipulate expression of these signaling components. Guide RNAs

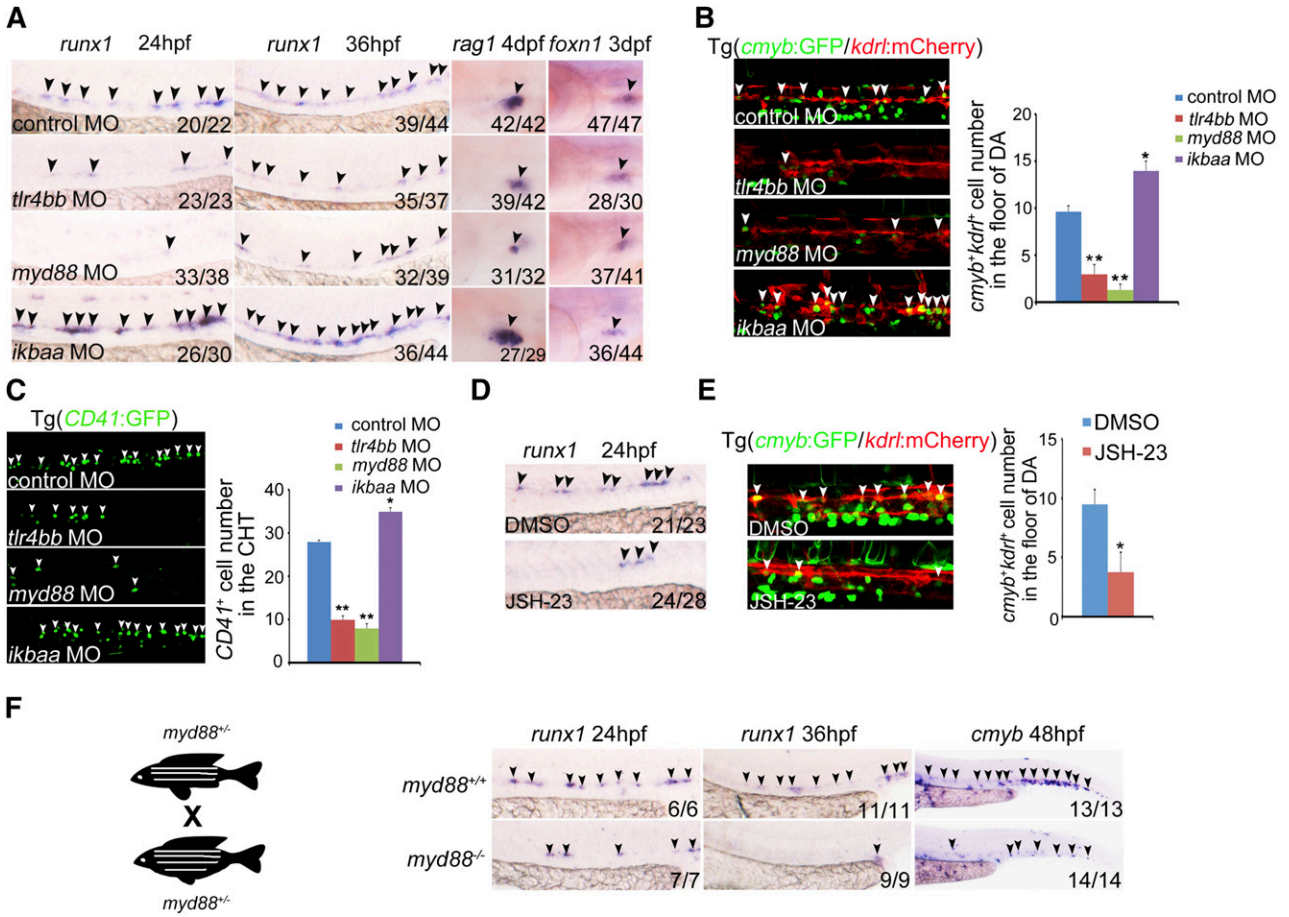

Figure 2. TLR4–MYD88–NF-κB signaling is essential for HSPC emergence. (A) *runx1* and *rag1* expression was decreased in *tlr4bb* and *myd88* morphants, but increased in *ikbaa* morphants; thymic epithelial cell marker *foxn1* expression was normal in all of these morphants. Black arrowheads mark expression of *runx1* in the AGM region at 24 hpf and 36 hpf, *rag1* in the thymus at 4 days post fertilization (dpf), and *foxn1* in the thymus at 3 dpf. (B) The number of $cmyb^+kdrl^+$ cells in Tg(*cmyb*:GFP/*kdrl*:mCherry) embryos was decreased in *tlr4bb* and *myd88* morphants and increased in *ikbaa* morphants. White arrowheads mark $cmyb^+kdrl^+$ cells in the AGM region at 36 hpf. Right panel, The quantification. Each bar represents the mean ± SEM of 3 independent samples. Each sample was composed of at least 5 embryos. $^*P < .05$, $^{**}P < .01$. (C) The hematopoietic cells in Tg(*CD41*:GFP) embryos were reduced in *tlr4bb* or *myd88* morphants and increased in *ikbaa* morphants. White arrowheads mark the *CD41* GFP^+ cells in the CHT region at 48 hpf. Right panel, The quantification of $CD41^+$ cells. Each bar represents the mean ± SEM of 3 independent samples. Each sample was composed of at least 5 embryos. $^*P < .05$, $^{**}P < .01$. (D) *runx1* expression was decreased in JSH-23–treated embryos at 36 hpf. Black arrowheads mark expression of *runx1* in the AGM region. (E) The population of $cmyb^+kdrl^+$ cells in Tg(*cmyb*:GFP/*kdrl*:mCherry) embryos was decreased in JSH-23–treated embryos. White arrowheads mark $cmyb^+kdrl^+$ cells in the AGM region at 36 hpf. Right panel, Quantification of $cmyb^+kdrl^+$ cells. Data are presented as mean ± SEM of 3 independent samples. Each sample was composed of at least 5 embryos. $^*P < .05$, $^{**}P < .01$. (F) The cartoon showed the incross between $myd88^{+/-}$ embryos. Right panels, The decreased expression of *runx1* and *cmyb* expression in $myd88^{-/-}$ embryos. Black arrowheads mark expression of *runx1* in the AGM region at 24 hpf and 36 hpf, and *cmyb* expression in the CHT region at 48 hpf.

targeting gene-specific promoters, together with a dead form of Cas9 fused with transcriptional repressor KRAB[43] (supplemental Figure 3A), were coinjected into zebrafish embryos at the 1-cell stage to achieve conditional repression of genes of interest. Transcriptional repression of TLR4-MyD88 (supplemental Figure 3B) remarkably reduced *runx1* expression and the number of $cmyb^+$ $kdrl^+$ cells in the AGM region and $CD41^+$ cells in the caudal hematopoietic tissue (CHT) region (supplemental Figure 3C-E).

To further support that inflammatory signaling is required for HSPC development, we treated embryos with JSH-23, a commonly used inhibitor for the nuclear translocation of NF-κB.[44] First, the efficiency of JSH-23 treatment was validated in zebrafish embryos. The nuclear p65 level was decreased in JSH-23–treated embryos (supplemental Figure 4A). Furthermore, the tail amputation assay also showed that the mpo^+ myeloid cell number was decreased at the wound region when treated with JSH-23 (supplemental Figure 4B), suggesting that the injury-induced inflammation response was attenuated by JSH-23 treatment. Then, similar HSPC defects were observed in JSH-23–treated embryos (Figure 2D-E). Given that we demonstrated that inflammatory signaling was necessary for HSPC emergence, we wondered whether it was also sufficient to promote this process. Knockdown of IκBaa, the NF-κB inhibitory protein that normally binds to NF-κB and prevents the translocation of NF-κB to the nucleus,[45] increased the number of HSPCs (Figure 2A-B). Consistently, the decreased expression of HSPC markers was also observed in the *myd88* mutants (Figure 2F).

To pinpoint the stage of HSPC development at which inflammatory signaling was required, we performed time-lapse live confocal imaging with *cmyb*:GFP/*kdrl*:mCherry double transgenic lines. The number of $cmyb^+kdrl^+$ cells was reduced at the onset of HSPC emergence at 30 to 36 hpf in inflammatory signaling-deficient embryos (supplemental Videos 1-3). In addition, *runx1* expression was reduced at 24 hpf, agreeing well with a defect in HE specification (Figure 2A,F). Taken together, these data demonstrated that proinflammatory signaling is required for HE-derived HSPC emergence in zebrafish embryos.

Endothelial cell–derived NF-κB mediates the TLR regulation of HSPC emergence

We went further to determine whether TLR4–MyD88–NF-κB regulation of HSPC development is mediated by NF-κB derived from

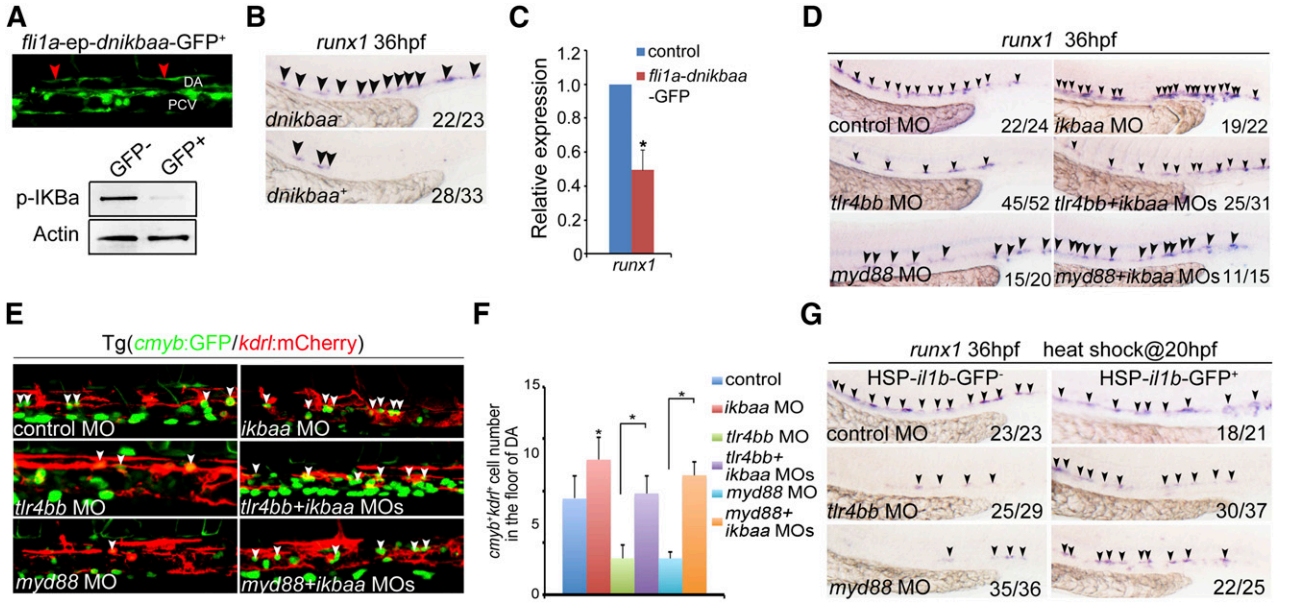

Figure 3. NF-κB derived from endothelial cells mediates the TLR regulation of HSPC emergence. (A) Top panel, Endothelial dnIκBaa-GFP$^+$ signals. Red arrowheads mark GFP signal in the endothelial cells. Bottom panels, The decreased expression of p-IKBa in *dnikbaa*$^-$ and *dnikbaa*$^+$ embryos. (B-C) Overexpression of *dnikbaa* in endothelial cells led to decreased expression of *runx1*. (D) Decreased expression of *runx1* at 36 hpf in *tlr4bb* or *myd88* morphants was rescued by coinjection of *ikbaa* MO. (E) The decreased population of *cmyb*$^+$ *kdrl*$^+$ cells in Tg(*cmyb*:GFP/*kdrl*:mCherry) embryos injected with *tlr4bb* or *myd88* MO, was rescued by coinjection with *ikbaa* MO. White arrowheads mark *cmyb*$^+$ *kdrl*$^+$ cells in the AGM region at 36 hpf. (F) Quantification of *cmyb*$^+$ *kdrl*$^+$ cells. Data are presented as mean ± SEM of 3 independent samples. Each sample was composed of at least 5 embryos. $^*P < .05$, $^{**}P < .01$. (G) Decreased expression of *runx1* at 36 hpf in *tlr4bb* or *myd88* morphants was rescued by the overexpression of *il1b* from 20 hpf.

endothelial cells rather than other sources. First, the western blotting result showed that the nuclear localization of NF-κB was indeed decreased in the *tlr4bb* or *myd88* morphants, whereas increased in *ikbaa* morphants (supplemental Figure 4C). Then, we generated a gateway construct driven by the *fli1a* promoter to express dominant-negative IκBaa (*dnikbaa*), which lacks the first 117 N-terminal nucleotides,[46] fused with GFP. The truncated IκBaa cannot be phosphorylated by the IκB kinase, and therefore prevents the nucleus translocation of NF-κB.[14] The endothelial GFP signals indicated the specific expression of *dnikbaa* (Figure 3A), and the phosphorylated level of IκBa was decreased in these GFP$^+$ embryos (Figure 3A). This endothelial-specific attenuation of NF-κB signaling mimicked the HSPC defects observed in *tlr4bb* or *myd88* morphants (Figure 3B-C). Importantly, coinjection of *ikbaa* MOs efficiently restored the decreased population of HSPCs and *il1b* expression in *tlr4bb* or *myd88* morphants (Figure 3D-F, supplemental Figure 4D). Furthermore, overexpression of *il1b* by heat shock treatment of a transgenic line with heat-shock–inducible *il1b* embryos [Tg(HSP-*il1b*-EGFP),[20] from 20 hpf, when the artery-vein specification has been accomplished] can also rescue the HSPC defects in the absence of *tlr4bb* or *myd88* (Figure 3G). Together, these data demonstrated that endothelial TLR4–MyD88–NF-κB signaling is both necessary and sufficient for HSPCs in zebrafish.

Because the earliest HSPCs are derived from the hemogenic endothelial cells in the dorsal aorta,[47,48] the observed HSPC defects in inflammatory signaling-deficient embryos were likely attributed to the defective vessel or artery specification. To explore this possibility, we examined expression of endothelial marker *kdrl* and arterial marker *ephrinB2*. Expression of these markers was not altered (supplemental Figure 5A-B), indicating a proper vessel development and artery-vein establishment. Similarly, we examined primitive hematopoiesis in these inflammatory signaling-deficient embryos. We found that expression of hemangioblast marker *scl*, erythroid marker *gata1*, and myeloid marker *l-plastin* was relatively normal, suggesting that primitive hematopoiesis was not affected (supplemental Figure 5C). In addition, TUNEL and BrdU staining showed no significant changes in the AGM region in the morphants, compared with control embryos (supplemental Figure 5D-E), implying that the observed HSPC defects were not caused by abnormal cell proliferation or excessive apoptosis.

Notch signaling functions downstream of inflammatory signaling to regulate HSPC emergence

TLR signaling has been reported to cooperate with Notch signaling to promote production of inflammatory cytokines, and Notch signaling acts upstream of Runx1 to specify HSPCs.[49-51] To explore the possible link between Notch signaling and inflammatory signaling in HSPC emergence, we examined expression of a panel of Notch target genes by qRT-PCR in the AGM region of inflammatory signaling-deficient zebrafish embryos. A significant reduction in expression of Notch target genes was observed specifically in *tlr4bb* or *myd88* morphants (Figure 4A, supplemental Figure 6A). Furthermore, the expression of *hey2* was also confirmed in the *myd88* mutants (Figure 4B). Consistently, using a Notch reporter transgenic line *tp1*:DsRed/*fli1a:*EGFP,[25] *tp1*$^+$*fli1a*$^+$ positive cells in the AGM region were greatly reduced (Figure 4C), suggesting that Notch activity was attenuated in these morphants. Repression of these inflammatory genes using dead Cas9 technology further confirmed this result (supplemental Figure 6B). Next, we investigated whether overexpression of Notch can rescue the HSPC defects in the morphants. Endothelial-derived Notch overexpression with *fli1a* promoter-driven Notch intracellular domain (NICD) efficiently rescued the number of *runx1*$^+$ cells in the AGM region in inflammatory signaling-defective embryos (Figure 4D). Together, endothelial Notch signaling is downstream of TLR4–MyD88–NF-κB–mediated inflammatory signaling to control the emergence of HSPCs in zebrafish embryos.

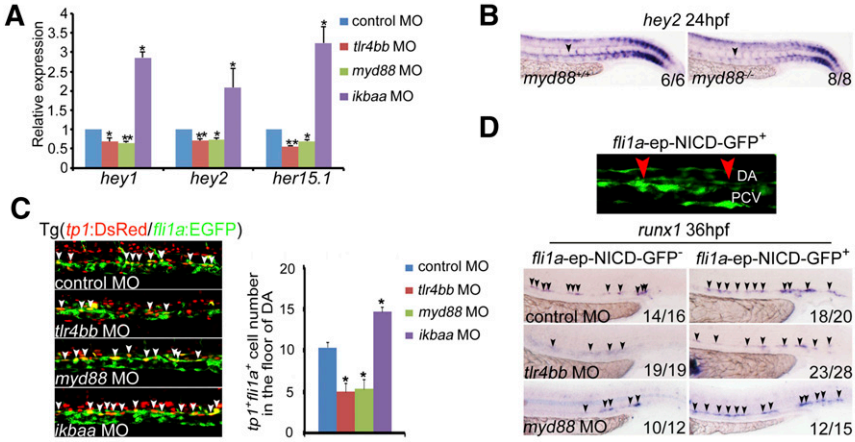

Figure 4. Notch signaling functions downstream of inflammatory signaling to regulate HSPC emergence. (A) qRT-PCR results from the dissected trunk region showed that expression of Notch target genes *hey1*, *hey2*, and *her15.1* was decreased in *tlr4bb* and *myd88* morphants and increased in *ikbaa* morphants at 28 hpf. Each bar represents the mean ± SEM of 3 independent samples. $^{*}P < .05$, $^{**}P < .01$. (B) *hey2* expression was decreased in *myd88*$^{-/-}$ embryos. Black arrowheads mark expression of *hey2* in the dorsal aorta at 24 hpf. (C) *tp1*$^{+}$*fli1a*$^{+}$ cells in Tg(*tp1*:DsRed/*fli1a*:EGFP) transgenic embryos were decreased in *tlr4bb* or *myd88* morphants and increased in *ikbaa* morphants. Left panels, Confocal images of the *tp1*$^{+}$*fli1a*$^{+}$ cells in the AGM region at 36 hpf, which were labeled by the white arrowheads. Right panel, Quantification of the *tp1*$^{+}$*fli1a*$^{+}$ cells. Each bar represents the mean ± SEM of 3 independent samples. Each sample was composed of at least 6 embryos. $^{*}P < .05$, $^{**}P < .01$. (D) Overexpression of NICD in endothelial cells partially rescued the HSPC defect in *tlr4bb* or *myd88* morphants. Top panel, The NICD-GFP^{+} signals. Bottom panels, The expression of *runx1* at 36 hpf in the embryos coinjected with *tlr4bb* or *myd88* MOs and *fli1a*-ep-NICD-GFP construct. Red arrowheads mark GFP signal in the endothelial cells. Black arrowheads mark the expression of *runx1* in the AGM region at 36 hpf.

Deficiency of inflammatory receptors leads to HSPC defects

NF-κB can respond to multiple inflammatory cytokines in innate immune responses. We thus examined whether attenuation of this cytokine-mediated signaling, including TNFα and G-CSF,[52,53] would cause similar HSPC defects as observed in TLR–NF-κB–deficient embryos. *runx1* expression was remarkably decreased in *tnfr2*- and *gcsfr*-deficient embryos by MO knockdown, compared with control embryos (Figure 5A). The number of *cmyb*$^{+}$*kdrl*$^{+}$ HSPCs in the AGM region was significantly reduced (Figure 5B). The HSPC phenotype in *gcsfr* morphants was consistent with a recent report by another group.[54] To demonstrate whether the cytokine signaling is mediated by NF-κB, we examined expression of *il1b* and found that *il1b* expression was decreased to the similar level as that in NF-κB–deficient embryos (Figure 5C), suggesting that the HSPC defects observed in *tnfr2*- and *gcsfr*-deficient embryos were likely attributed to dysregulated NF-κB signaling. Importantly, coinjection of *ikbaa* MO efficiently restored the decreased population of HSPCs in these morphants, indicating that NF-κB acts downstream of inflammatory cytokine signaling (Figure 5D). Taken together, these data support that inflammatory cytokines activate NF-κB signaling to control HE and HSPC specification.

Consistently, both the expression of Notch targets and the number of *tp1*$^{+}$*fli1a*$^{+}$ cells in the AGM region were greatly reduced in these inflammatory receptor-defective embryos (supplemental Figure 7A-C). Furthermore, the endothelial-derived NICD overexpression efficiently rescued the population of *runx1*$^{+}$ cells in the AGM region in inflammatory signaling-defective embryos (supplemental Figure 7D). Together, endothelial Notch signaling also functions downstream of inflammatory signaling to control the emergence of HSPCs in zebrafish embryos.

To determine which subset of the myeloid lineages is responsible for the production of inflammatory cytokines, we used *pu.1* MO which

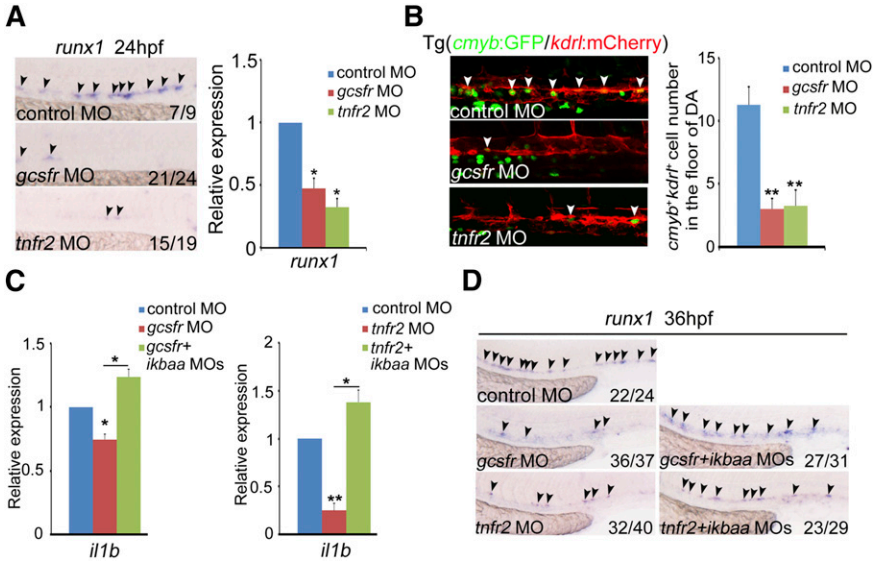

Figure 5. The deficiency of inflammatory receptors leads to HSPC defects. (A) Expression of HSPC marker *runx1* was decreased in *mcsfr*, *gcsfr*, and *tnfr2* morphants at 24 hpf. Black arrowheads labeled expression of *runx1* in the AGM region. (B) Fluorescence-labeled hemogenic endothelial cells were decreased in Tg(*cmyb*:GFP/*kdrl*:mCherry) embryos injected with *gcsfr* or *tnfr2* MO at 36 hpf. White arrowheads mark *cmyb*$^{+}$*kdrl*$^{+}$ cells in the AGM region. Each bar represents the mean ± SEM of 3 independent samples. Each sample was composed of at least 5 embryos. $^{**}P < .01$. (C) qRT-PCR analysis of the NF-κB target gene *il1b* showed that the decreased expression of *il1b* in *gcsfr* and *tnfr2* morphants at 36 hpf were rescued by coinjection of *ikbaa* MO. Each bar represents the mean ± SEM of 3 independent samples. $^{*}P < .05$, $^{**}P < .01$. (D) The decreased expression of HSPC marker *runx1* in *gcsfr* and *tnfr2* morphants were rescued by coinjection of *ikbaa* MO. Black arrowheads mark *runx1* expression in the AGM region at 36 hpf.

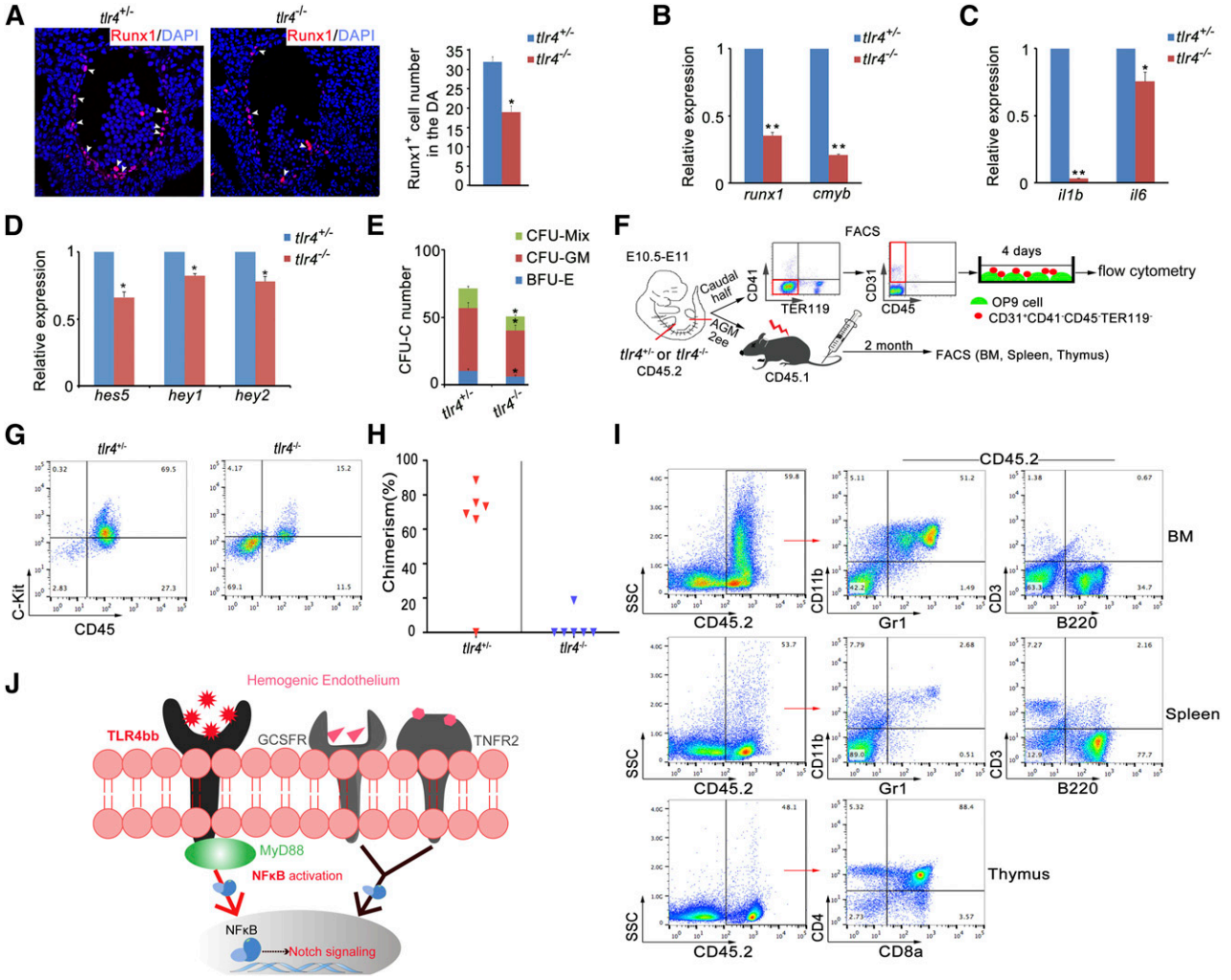

Figure 6. Inflammatory signaling plays an evolutionarily conserved role in mouse definitive hematopoiesis. (A) Immunofluorescence of Runx1 in the E10.5 AGM region of *tlr4*$^{+/-}$ and *tlr4*$^{-/-}$ embryos. Right panel, The quantification of Runx1^{+} cells in AGM region on the sections (*tlr4*$^{+/-}$, n = 3; *tlr4*$^{-/-}$, n = 3). (B-D) qRT-PCR analysis showed attenuated expression of HSC markers (B), NF-κB signaling target genes (C), and Notch target genes (D), respectively. (E) CFC assay of AGM regions showed the numbers of CFU-Mix, CFU-GM, and BFU-E were decreased in *tlr4*$^{-/-}$ embryos. One embryo equivalent was used. (F) The scheme of cell sorting and HSC transplantation assay in mouse embryos. (G) Flow cytometry results showed an increased amount of C-Kit^{+}CD45^{+} cells in *tlr4*$^{-/-}$ embryos after 4 days of OP9 coculture. (H) Donor-derived chimerism in recipients. Symbols represent the donor chimerism in bone marrow of each recipient at 2 months posttransplantation. (I) The donor-derived multilineage reconstitution was shown by the presence of CD45.2 cells in the myeloid (Gr1^{+}/CD11b^{+}), B lymphoid (B220^{+}), and T lymphoid (CD3^{+}, or CD4^{+}/CD8^{+}) populations of bone marrow, spleen, and thymus in a representative recipient at 2 months posttransplantation. (J) Model of inflammatory signaling during HSPC emergence. The inflammatory signals were required to activate NF-κB–Notch signaling in the hemogenic endothelial cells, and then regulate HSPC development. (B-E) Each bar represents the mean ± SEM of 3 independent samples. *$P < .05$, **$P < .01$.

can eliminate all myeloid lineages in zebrafish, *irf8* MO which attenuates macrophages, and *cebp1* MO which decreases neutrophils. The *runx1* expression was not much affected in *irf8* knockdown embryos, whereas decreased in *pu.1* and *cebp1* knockdown embryos (supplemental Figure 8A-B), suggesting that neutrophils are the main source for inflammatory cytokines responsible for HSPC emergence, consistent with the findings published recently.[13,14]

Inflammatory signaling plays an evolutionarily conserved role in mouse definitive hematopoiesis

To determine whether inflammatory signaling is evolutionarily conserved in HSPC emergence in mammals, we examined the AGM region of *tlr4*$^{-/-}$ knockout mice.[55] Immunofluorescence analysis showed that Runx1 expression was severely attenuated in the AGM (Figure 6A). qRT-PCR confirmed decreased levels of *runx1* and *cmyb*, as well as downregulated expression of *il1b* and *il6*, in NF-κB signaling (Figure 6B-C). As observed in zebrafish, expression of Notch target genes was also decreased (Figure 6D). The colony-forming unit-cell (CFU-C) assay showed compromised colony formation abilities of AGM tissues in *tlr4*$^{-/-}$ mice (Figure 6E). To test whether inflammatory signaling acts on endothelial cells cell-autonomously in mice, endothelial cells (CD31^{+}CD41^{-}CD45^{-}TER119^{-})[56] from the AGM tissues in *tlr4*$^{+/-}$ or *tlr4*$^{-/-}$ were cultured for 4 days, then flow cytometry was performed (Figure 6F). The C-Kit^{+}CD45^{+} hematopoietic cells were significantly decreased in *tlr4*$^{-/-}$ embryos (Figure 6G). The HSC transplantation is widely accepted as the most reliable assay for HSC activity. Five of 6 recipients were reconstituted after 2 months when transplanted with cells from tlr4$^{+/-}$ embryos, whereas only 1 of 6 reconstituted when transplanted with cells from tlr4$^{-/-}$ embryos (Figure 6H-I). Together, these data suggest that the role of inflammatory signaling in HSPC emergence is evolutionarily conserved in mammals.

Discussion

Many if not all developmental signaling pathways during developmental hematopoiesis and homeostasis have been identified. Inflammatory signaling has been well studied in infection and inflammation, but its physiological and developmental roles are poorly understood. In the present study, we have demonstrated that inflammatory signaling plays a highly conserved role in HSPC emergence in zebrafish and mice by investigating the expression pattern, requirement for HSPC specification, and regulatory mechanisms. Inflammatory signaling functions upstream of Notch signaling pathway via NF-κB. Our findings strongly support that proinflammatory signaling is a common master regulator of HSPC emergence and is shared by normal hematopoiesis and stress hematopoiesis in vertebrates.

The relationship between NF-κB and Notch is controversial and has been studied in different systems. The Notch signaling pathway is essential to maintain HSPC homeostasis by regulating the inflammatory signaling level in the bone marrow niche because inhibition of Notch signaling activates NF-κB via mir-155 and leads to myeloproliferation.[57] On the one hand, Notch may prevent the NF-κB activation by directly interacting with NF-κB in the nucleus.[58] On the other hand, Notch signaling has been reported to activate NF-κB[59,60] as well. In hematopoietic progenitor cells, Notch1 has been shown to regulate NF-κB activity through transcriptional regulation of NF-κB subunits.[61] In the T-cell leukemia, the Notch/Hes1 pathway sustains the NF-κB activation by negatively regulating IκB kinase.[62] Furthermore, the cooperation of Notch3 and canonical NF-κB signaling pathways can regulate Foxp3 transcription to maintain the regulatory T-cell homeostasis and function.[63] In this work, we identified the NF-κB regulation of the Notch signaling pathway by upregulating Notch signaling at the onset of definitive hematopoiesis, which is consistent with the NF-κB–dependent activation of Notch in endothelial cells[64] and peripheral lymphoid tissues.[65] Further studies are warranted to fully characterize the interaction between these 2 pathways in HE and HSPC specification.

Baseline inflammatory signaling might be crucial for the emergence of HSPCs under the physiological condition in that a low level of inflammatory signaling promotes HSPC specification or "priming." Once in demand, that is, in response to infection, inflammatory signaling will rapidly induce the programming for cytokine production within the earliest HSPCs, and efficiently instruct HSPC differentiation into effector immune cells, such as myeloid and lymphoid cells.[8,66] However, the sources of endogenous TLR ligands and inflammatory cytokines during normal hematopoiesis remain unclear. It is possible that the reported heat shock proteins and signals from damaged or stressed cells[67] firstly induce the TLR4–NF-κB pathway during normal embryonic hematopoiesis, and then activate the Notch pathway to regulate the HSPC emergence.

In conclusion, our results support that proinflammatory signaling is a novel and potent regulator during HSPC emergence and is shared by normal and stress hematopoiesis in vertebrates. This may prove to be a useful theoretical basis in treating patients with bone marrow failure or following transplantation with clinically applicable cytokines and point to a new strategy for developing a new protocol for in vitro generation and expansion of inducible HSPCs by modulation of inflammatory signaling.

Note added in proof. During the preparation of the revision for this work, 3 recent publications reported that proinflammatory signaling mediated by TNFα or interferons plays an essential role in HSPC development in zebrafish and mouse embryos,[12-14] consistent with our findings here.

Acknowledgments

The authors thank Dangsheng Li and Zilong Wen for helpful discussions and/or critical reading of the paper. The authors also thank Zilong Wen and Jing-Wei Xiong for providing the reagents used in this work.

This work was supported by grants from the National Basic Research Program of China (2010CB945300, 2011CB943900), the National Natural Science Foundation of China (31271570, 31425016), and the Strategic Priority Research Program of the Chinese Academy of Sciences (CAS) (XDA01010110).

Authorship

Contribution: Q.H., C.Z., L.W., P.Z., D.M., and J.L. performed the experiments; F.L. conceived the project, analyzed the data, and wrote the paper; and all authors read and approved the final manuscript.

Conflict-of-interest disclosure: The authors declare no competing financial interests.

Correspondence: Feng Liu, State Key Laboratory of Biomembrane and Membrane Biotechnology, Institute of Zoology, Chinese Academy of Sciences, Beijing 100101, China; e-mail: liuf@ioz.ac.cn.

References

1. Jaffredo T, Gautier R, Eichmann A, Dieterlen-Lièvre F. Intraaortic hemopoietic cells are derived from endothelial cells during ontogeny. *Development.* 1998;125(22):4575-4583.
2. Jaffredo T, Bollerot K, Sugiyama D, Gautier R, Drevon C. Tracing the hemangioblast during embryogenesis: developmental relationships between endothelial and hematopoietic cells. *Int J Dev Biol.* 2005; 49(2-3):269-277.
3. Kaimakis P, Crisan M, Dzierzak E. The biochemistry of hematopoietic stem cell development. *Biochim Biophys Acta.* 2013; 1830(2):2395-2403.
4. Gordon-Keylock S, Medvinsky A. Endothelio-hematopoietic relationship: getting closer to the beginnings. *BMC Biol.* 2011;9:88.
5. Bertrand JY, Chi NC, Santoso B, Teng S, Stainier DY, Traver D. Haematopoietic stem cells derive directly from aortic endothelium during development. *Nature.* 2010;464(7285): 108-111.
6. Boisset JC, van Cappellen W, Andrieu-Soler C, Galjart N, Dzierzak E, Robin C. In vivo imaging of haematopoietic cells emerging from the mouse aortic endothelium. *Nature.* 2010;464(7285): 116-120.
7. Kissa K, Herbomel P. Blood stem cells emerge from aortic endothelium by a novel type of cell transition. *Nature.* 2010;464(7285):112-115.
8. Mossadegh-Keller N, Sarrazin S, Kandalla PK, et al. M-CSF instructs myeloid lineage fate in single haematopoietic stem cells. *Nature.* 2013; 497(7448):239-243.
9. Klein Wolterink RG, Serafini N, van Nimwegen M, et al. Essential, dose-dependent role for the transcription factor Gata3 in the development of IL-5+ and IL-13+ type 2 innate lymphoid cells. *Proc Natl Acad Sci USA.* 2013;110(25): 10240-10245.
10. Essers MA, Offner S, Blanco-Bose WE, et al. IFNalpha activates dormant haematopoietic stem cells in vivo. *Nature.* 2009;458(7240):904-908.
11. Baldridge MT, King KY, Boles NC, Weksberg DC, Goodell MA. Quiescent haematopoietic stem cells are activated by IFN-gamma in response to chronic infection. *Nature.* 2010;465(7299): 793-797.
12. Sawamiphak S, Kontarakis Z, Stainier DY. Interferon gamma signaling positively regulates hematopoietic stem cell emergence. *Dev Cell.* 2014;31(5):640-653.

13. Li Y, Esain V, Teng L, et al. Inflammatory signaling regulates embryonic hematopoietic stem and progenitor cell production. *Genes Dev.* 2014;28(23):2597-2612.
14. Espín-Palazón R, Stachura DL, Campbell CA, et al. Proinflammatory signaling regulates hematopoietic stem cell emergence. *Cell.* 2014; 159(5):1070-1085.
15. Robin C, Ottersbach K, Durand C, et al. An unexpected role for IL-3 in the embryonic development of hematopoietic stem cells. *Dev Cell.* 2006;11(2):171-180.
16. Orelio C, Haak E, Peeters M, Dzierzak E. Interleukin-1-mediated hematopoietic cell regulation in the aorta-gonad-mesonephros region of the mouse embryo. *Blood.* 2008; 112(13):4895-4904.
17. Lu X, Li X, He Q, et al. miR-142-3p regulates the formation and differentiation of hematopoietic stem cells in vertebrates. *Cell Res.* 2013;23(12): 1356-1368.
18. North TE, Goessling W, Walkley CR, et al. Prostaglandin E2 regulates vertebrate haematopoietic stem cell homeostasis. *Nature.* 2007;447(7147):1007-1011.
19. Lawson ND, Weinstein BM. In vivo imaging of embryonic vascular development using transgenic zebrafish. *Dev Biol.* 2002;248(2): 307-318.
20. Yan B, Han P, Pan L, et al. IL-1β and reactive oxygen species differentially regulate neutrophil directional migration and Basal random motility in a zebrafish injury-induced inflammation model. *J Immunol.* 2014;192(12):5998-6008.
21. Lin HF, Traver D, Zhu H, et al. Analysis of thrombocyte development in CD41-GFP transgenic zebrafish. *Blood.* 2005;106(12): 3803-3810.
22. Renshaw SA, Loynes CA, Trushell DM, Elworthy S, Ingham PW, Whyte MK. A transgenic zebrafish model of neutrophilic inflammation. *Blood.* 2006; 108(13):3976-3978.
23. Hall C, Flores MV, Storm T, Crosier K, Crosier P. The zebrafish lysozyme C promoter drives myeloid-specific expression in transgenic fish. *BMC Dev Biol.* 2007;7:42.
24. van der Vaart M, van Soest JJ, Spaink HP, Meijer AH. Functional analysis of a zebrafish myd88 mutant identifies key transcriptional components of the innate immune system. *Dis Model Mech.* 2013;6(3):841-854.
25. Parsons MJ, Pisharath H, Yusuff S, et al. Notch-responsive cells initiate the secondary transition in larval zebrafish pancreas. *Mech Dev.* 2009; 126(10):898-912.
26. Sepulcre MP, Alcaraz-Pérez F, López-Muñoz A, et al. Evolution of lipopolysaccharide (LPS) recognition and signaling: fish TLR4 does not recognize LPS and negatively regulates NF-kappaB activation. *J Immunol.* 2009;182(4):1836-1845.
27. Alcaraz-Pérez F, Mulero V, Cayuela ML. Application of the dual-luciferase reporter assay to the analysis of promoter activity in Zebrafish embryos. *BMC Biotechnol.* 2008;8:81.
28. Tam SJ, Richmond DL, Kaminker JS, et al. Death receptors DR6 and TROY regulate brain vascular development. *Dev Cell.* 2012;22(2):403-417.
29. Huang T, Cui J, Li L, Hitchcock PF, Li Y. The role of microglia in the neurogenesis of zebrafish retina. *Biochem Biophys Res Commun.* 2012; 421(2):214-220.
30. Clay H, Davis JM, Beery D, Huttenlocher A, Lyons SE, Ramakrishnan L. Dichotomous role of the macrophage in early Mycobacterium marinum infection of the zebrafish. *Cell Host Microbe.* 2007;2(1):29-39.
31. Li L, Jin H, Xu J, Shi Y, Wen Z. Irf8 regulates macrophage versus neutrophil fate during zebrafish primitive myelopoiesis. *Blood.* 2011; 117(4):1359-1369.
32. Kitaguchi T, Kawakami K, Kawahara A. Transcriptional regulation of a myeloid-lineage specific gene lysozyme C during zebrafish myelopoiesis. *Mech Dev.* 2009;126(5-6):314-323.
33. Villefranc JA, Amigo J, Lawson ND. Gateway compatible vectors for analysis of gene function in the zebrafish. *Dev Dyn.* 2007;236(11):3077-3087.
34. Wei Y, Ma D, Gao Y, Zhang C, Wang L, Liu F. Ncor2 is required for hematopoietic stem cell emergence by inhibiting Fos signaling in zebrafish. *Blood.* 2014;124(10):1578-1585.
35. Wang L, Zhang P, Wei Y, Gao Y, Patient R, Liu F. A blood flow-dependent klf2a-NO signaling cascade is required for stabilization of hematopoietic stem cell programming in zebrafish embryos. *Blood.* 2011;118(15):4102-4110.
36. Ma D, Wang L, Wang S, Gao Y, Wei Y, Liu F. Foxn1 maintains thymic epithelial cells to support T-cell development via mcm2 in zebrafish. *Proc Natl Acad Sci USA.* 2012;109(51):21040-21045.
37. Wang L, Liu T, Xu L, et al. Fev regulates hematopoietic stem cell development via ERK signaling. *Blood.* 2013;122(3):367-375.
38. Renaud O, Herbomel P, Kissa K. Studying cell behavior in whole zebrafish embryos by confocal live imaging: application to hematopoietic stem cells. *Nat Protoc.* 2011;6(12):1897-1904.
39. Covassin L, Amigo JD, Suzuki K, Teplyuk V, Straubhaar J, Lawson ND. Global analysis of hematopoietic and vascular endothelial gene expression by tissue specific microarray profiling in zebrafish. *Dev Biol.* 2006;299(2):551-562.
40. Ng CE, Yokomizo T, Yamashita N, et al. A Runx1 intronic enhancer marks hemogenic endothelial cells and hematopoietic stem cells. *Stem Cells.* 2010;28(10):1869-1881.
41. Lam EY, Hall CJ, Crosier PS, Crosier KE, Flores MV. Live imaging of Runx1 expression in the dorsal aorta tracks the emergence of blood progenitors from endothelial cells. *Blood.* 2010; 116(6):909-914.
42. Takeuchi O, Akira S. Pattern recognition receptors and inflammation. *Cell.* 2010;140(6): 805-820.
43. Kearns NA, Genga RM, Enuameh MS, Garber M, Wolfe SA, Maehr R. Cas9 effector-mediated regulation of transcription and differentiation in human pluripotent stem cells. *Development.* 2014;141(1):219-223.
44. Koo JW, Russo SJ, Ferguson D, Nestler EJ, Duman RS. Nuclear factor-kappaB is a critical mediator of stress-impaired neurogenesis and depressive behavior. *Proc Natl Acad Sci USA.* 2010;107(6):2669-2674.
45. Correa RG, Tergaonkar V, Ng JK, Dubova I, Izpisua-Belmonte JC, Verma IM. Characterization of NF-kappa B/I kappa B proteins in zebra fish and their involvement in notochord development. *Mol Cell Biol.* 2004;24(12):5257-5268.
46. Abbas S, Abu-Amer Y. Dominant-negative IkappaB facilitates apoptosis of osteoclasts by tumor necrosis factor-alpha. *J Biol Chem.* 2003; 278(22):20077-20082.
47. Zhang C, Patient R, Liu F. Hematopoietic stem cell development and regulatory signaling in zebrafish. *Biochim Biophys Acta.* 2013;1830(2): 2370-2374.
48. Clements WK, Traver D. Signalling pathways that control vertebrate haematopoietic stem cell specification. *Nat Rev Immunol.* 2013;13(5): 336-348.
49. Hu X, Chung AY, Wu I, et al. Integrated regulation of Toll-like receptor responses by Notch and interferon-gamma pathways. *Immunity.* 2008; 29(5):691-703.
50. Burns CE, Traver D, Mayhall E, Shepard JL, Zon LI. Hematopoietic stem cell fate is established by the Notch-Runx pathway. *Genes Dev.* 2005; 19(19):2331-2342.
51. Nakagawa M, Ichikawa M, Kumano K, et al. AML1/Runx1 rescues Notch1-null mutation-induced deficiency of para-aortic splanchnopleural hematopoiesis. *Blood.* 2006; 108(10):3329-3334.
52. Baud V, Karin M. Signal transduction by tumor necrosis factor and its relatives. *Trends Cell Biol.* 2001;11(9):372-377.
53. Roca FJ, Mulero I, López-Muñoz A, et al. Evolution of the inflammatory response in vertebrates: fish TNF-alpha is a powerful activator of endothelial cells but hardly activates phagocytes. *J Immunol.* 2008;181(7):5071-5081.
54. Stachura DL, Svoboda O, Campbell CA, et al. The zebrafish granulocyte colony-stimulating factors (Gcsfs): 2 paralogous cytokines and their roles in hematopoietic development and maintenance. *Blood.* 2013;122(24):3918-3928.
55. Poltorak A, He X, Smirnova I, et al. Defective LPS signaling in C3H/HeJ and C57BL/10ScCr mice: mutations in Tlr4 gene. *Science.* 1998;282(5396): 2085-2088.
56. Li Z, Lan Y, He W, et al. Mouse embryonic head as a site for hematopoietic stem cell development. *Cell Stem Cell.* 2012;11(5):663-675.
57. Wang L, Zhang H, Rodriguez S, et al. Notch-dependent repression of miR-155 in the bone marrow niche regulates hematopoiesis in an NF-κB-dependent manner. *Cell Stem Cell.* 2014; 15(1):51-65.
58. Guan E, Wang J, Laborda J, Norcross M, Baeuerle PA, Hoffman T. T cell leukemia-associated human Notch/translocation-associated Notch homologue has I kappa B-like activity and physically interacts with nuclear factor-kappa B proteins in T cells. *J Exp Med.* 1996;183(5):2025-2032.
59. Oswald F, Liptay S, Adler G, Schmid RM. NF-kappaB2 is a putative target gene of activated Notch-1 via RBP-Jkappa. *Mol Cell Biol.* 1998; 18(4):2077-2088.
60. Bellavia D, Campese AF, Alesse E, et al. Constitutive activation of NF-kappaB and T-cell leukemia/lymphoma in Notch3 transgenic mice. *EMBO J.* 2000;19(13):3337-3348.
61. Cheng P, Zlobin A, Volgina V, et al. Notch-1 regulates NF-kappaB activity in hemopoietic progenitor cells. *J Immunol.* 2001;167(8): 4458-4467.
62. Espinosa L, Cathelin S, D'Altri T, et al. The Notch/Hes1 pathway sustains NF-κB activation through CYLD repression in T cell leukemia. *Cancer Cell.* 2010;18(3):268-281.
63. Barbarulo A, Grazioli P, Campese AF, et al. Notch3 and canonical NF-kappaB signaling pathways cooperatively regulate Foxp3 transcription. *J Immunol.* 2011;186(11): 6199-6206.
64. Johnston DA, Dong B, Hughes CC. TNF induction of jagged-1 in endothelial cells is NFkappaB-dependent. *Gene.* 2009;435(1-2):36-44.
65. Bash J, Zong WX, Banga S, et al. Rel/NF-kappaB can trigger the Notch signaling pathway by inducing the expression of Jagged1, a ligand for Notch receptors. *EMBO J.* 1999;18(10): 2803-2811.
66. Zhao JL, Ma C, O'Connell RM, et al. Conversion of danger signals into cytokine signals by hematopoietic stem and progenitor cells for regulation of stress-induced hematopoiesis. *Cell Stem Cell.* 2014;14(4):445-459.
67. Akira S, Takeda K, Kaisho T. Toll-like receptors: critical proteins linking innate and acquired immunity. *Nat Immunol.* 2001;2(8):675-680.